Electronic Supplementary Material (ESI) for Dalton Transactions.
This journal is © The Royal Society of Chemistry 2020

Influence of magnetic dilution on relaxation processes in a solid solution comprising tetrahedral Co/Zn^{II} complexes

Magdalena Ceglarska[a], Olaf Stefańczyk[b], Shin-ichi Ohkoshi[b], and Anna M. Majcher-Fitas[*a]

[a]Faculty of Physics, Astronomy and Applied Computer Science, Jagiellonian University, Łojasiewicza 11, 30–348 Krakow, Poland

[b]Department of Chemistry, School of Science, The University of Tokyo, 7-3-1 Hongo, Bunkyo-ku, Tokyo 113-0033, Japan

Electronic Supplementary Information

Structural analysis of solid-solutions

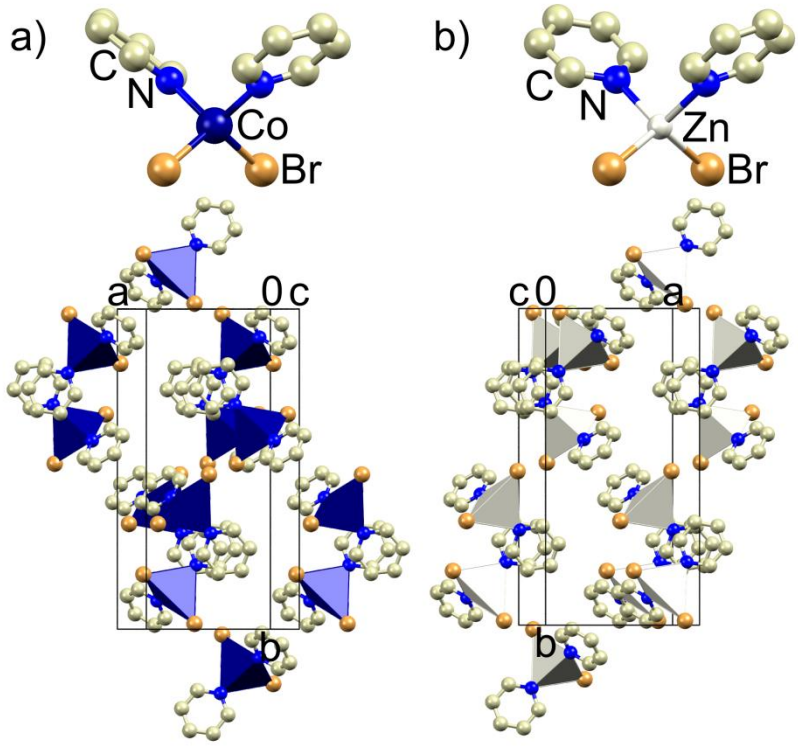

Figure S1. Single crystal X-ray structure of **1-Co**[S1] (a) and **0-Co**[S2] (b).

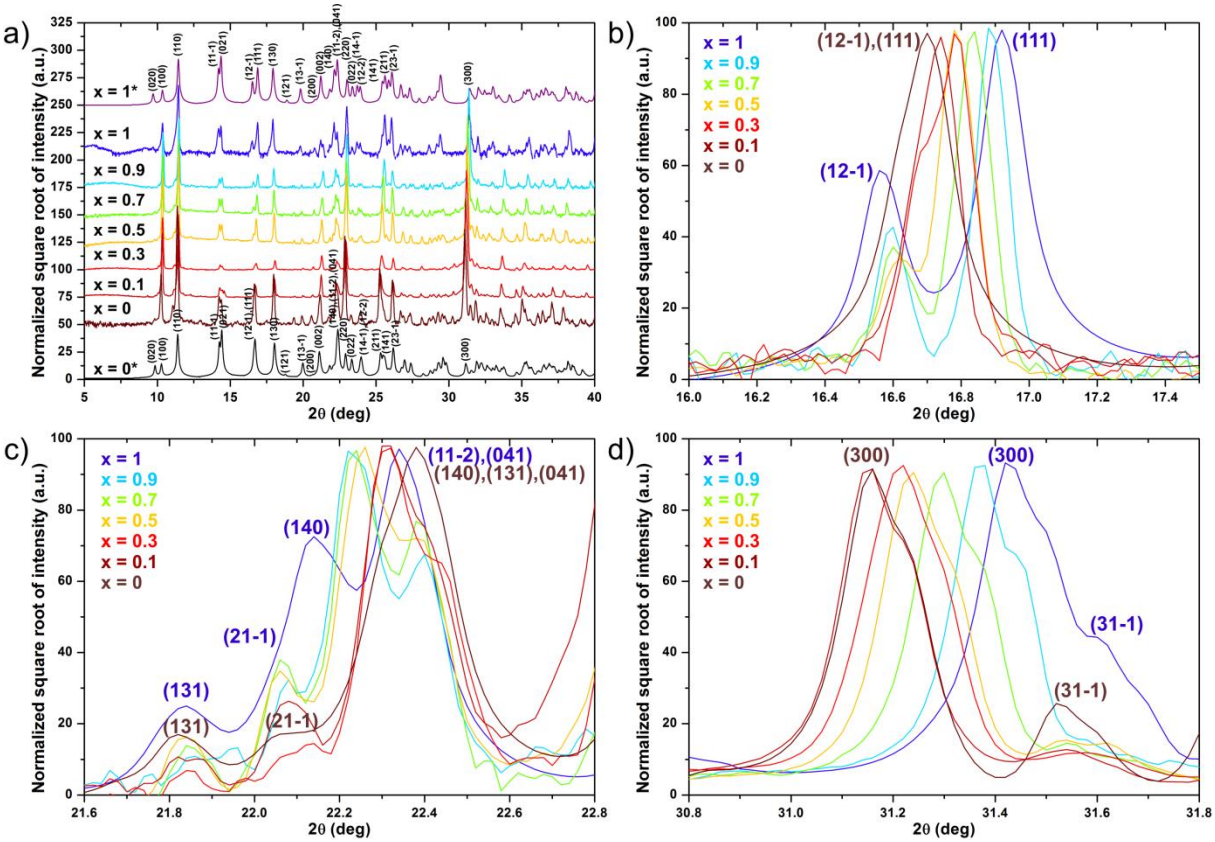

Figure S2. a) Measured powder X-ray diffractograms for solid-solutions and simulated ones for single crystal structures of **1-Co** and **0-Co**. In-depth analysis of the normalized square root of intensity for peaks around 16.8° (b), 22.3° (c) and 31.3° (d) 2-theta angles.

Table S1. Analysis of Co:Zn ratio based on PXRD measurement for solid-solutions.

$Co_xZn_{1-x}Br_2(pyridine)_2$	(300) peak position	Co:Zn ratio
***x* = 1**	31.41°	10:0
***x′* = 0.9**	31.38°	9:1
***x′* = 0.7**	31.30°	6:4
***x′* = 0.5**	31.23°	3:7
***x′* = 0.3**	31.21°	2:8
***x′* = 0.1**	31.16°	5:95
***x* = 0**	31.15°	0:10

Comparison of elemental analysis results and ICP+MS.

Table S2. Microelemental analysis and ICP+MS results for pure compounds (**1-Co** and **0-Co**) and solid-solutions (***x'*= 0.1 - 0.9**).

Compound	M_W (g/mol)		Microelemental analysis				ICP+MS			Co:Zn ratio	
			C (%)	H (%)	N (%)	Br (%)	Br (%)	Co (%)	Zn (%)	EIM[a]	MGT[b]
$\mathbf{Co}_{0.93}\mathbf{Zn}_{0.07}\mathbf{(py)_2Br_2}$ $C_{10}H_{10}Br_2Co_{0.93}N_2Zn_{0.07}$ (**x = 0.9**)	377.4	Calc.	31.83	2.67	7.42	42.35		14.52	1.21	**0.93**	**0.78**
		Found	31.73	2.82	7.51	42.44	42.16	14.54	1.19		
$\mathbf{Co}_{0.67}\mathbf{Zn}_{0.33}\mathbf{(py)_2Br_2}$ $C_{10}H_{10}Br_2Co_{0.7}N_2Zn_{0.33}$ (**x = 0.7**)	379.1	Calc.	31.68	2.66	7.39	42.16		10.42	5.69	**0.67**	**0.52**
		Found	31.64	2.79	7.46	42.18	42.03	10.39	5.71		
$\mathbf{Co}_{0.41}\mathbf{Zn}_{0.59}\mathbf{(py)_2Br_2}$ $C_{10}H_{10}Br_2Co_{0.41}N_2Zn_{0.59}$ (**x = 0.5**)	380.8	Calc.	31.54	2.65	7.36	41.97		6.35	10.14	**0.41**	**0.34**
		Found	31.48	2.84	7.37	42.05	41.89	6.45	10.02		
$\mathbf{Co}_{0.24}\mathbf{Zn}_{0.76}\mathbf{(py)_2Br_2}$ $C_{10}H_{10}Br_2Co_{0.24}N_2Zn_{0.76}$ (**x = 0.3**)	381.9	Calc.	31.45	2.64	7.34	41.85		3.70	13.02	**0.24**	**0.23**
		Found	31.40	2.67	7.35	41.90	41.81	3.76	12.95		
$\mathbf{Co}_{0.06}\mathbf{Zn}_{0.94}\mathbf{(py)_2Br_2}$ $C_{10}H_{10}Br_2Co_{0.06}N_2Zn_{0.94}$ (**x = 0.1**)	383.0	Calc.	31.36	2.63	7.31	41.72		0.92	16.05	**0.06**	**0.05**
		Found	31.31	2.79	7.22	41.83	41.71	0.86	16.12		

[a] Co:Zn molar ratio obtained from the collective results of elemental analysis and ICP+MS

[b] Co:Zn molar ratio obtained from the value of magnetization at 1.8 K in 50 kOe compared with the same value for **1-Co**.

Fourier-Transform Infrared (FTIR) spectroscopy for pure and solid-solutions

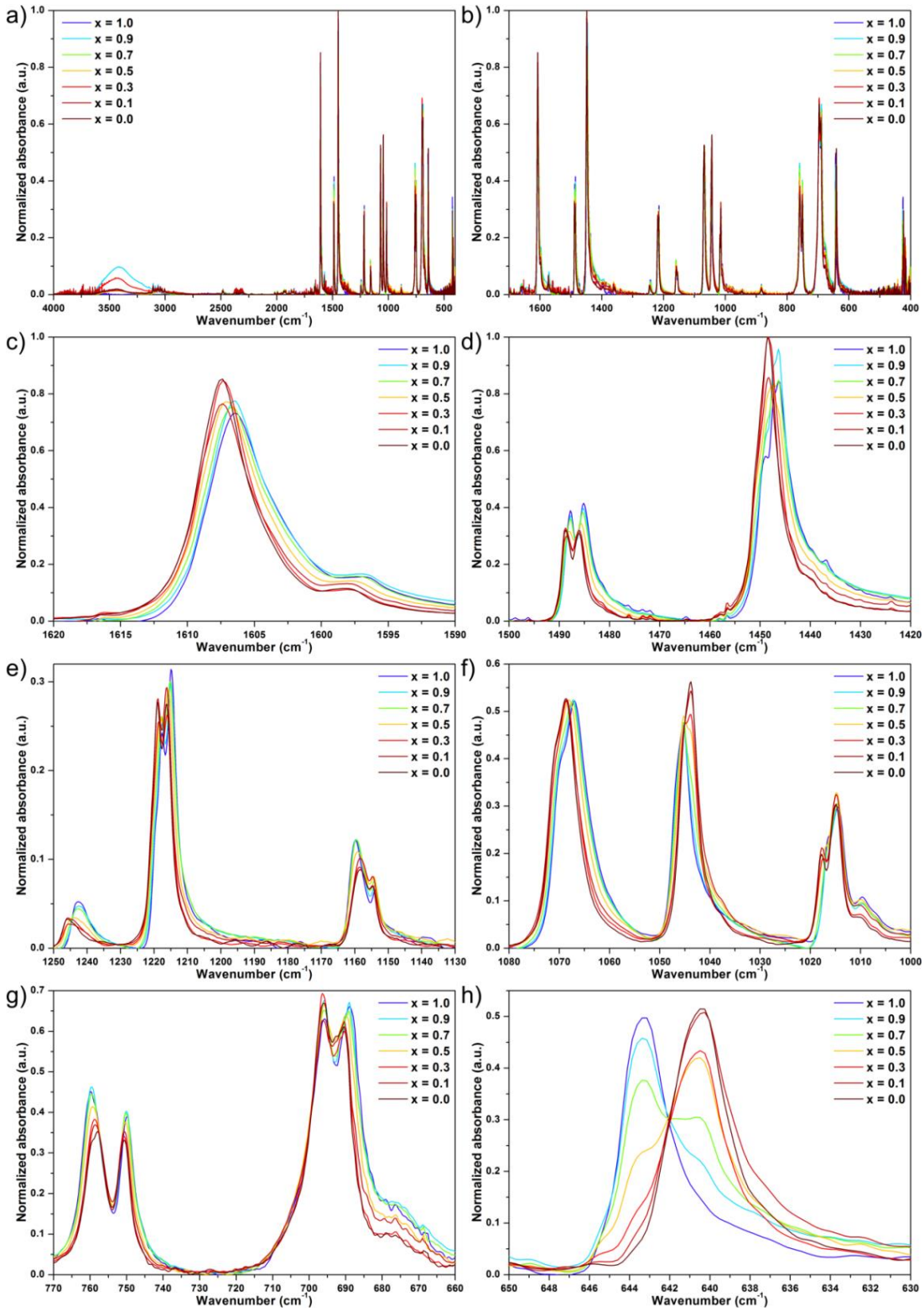

Figure S3. FTIR measurements results for pure compounds (**1-Co** and **0-Co**) and solid-solutions (**Co_xZn_{1-x}**).

5. Solid state UV-Vis-NIR diffuse-reflectance spectroscopy for pure and solid-solutions.

It is worth to emphasize that absorption bands in 20000 - 5000 cm^{-1} energy range (VIS-NIR) corresponds to d-d excitations of distorted tetrahedral d^7 cobalt(II) centre with C_{2v} symmetry.[S1] The Co(II) centre in the ideal tetrahedral (T_d) ligand field gives a $^4A_2$ ground state and $^4T_2$, $^4T_1(^4F)$, and $^4T_1(^4P)$ excited ones, listed in order of augmenting energy, which can generate three intense absorptions around 6000, 9000 and 16000 cm^{-1} in the UV-Vis-NIR spectrum. The crystal structures of pure compounds (**1-Co** and **0-Co**) and solid-solutions (**Co_xZn_{1-x}**) contain metal centres with C_{2v} local symmetry which lower splits the T_d d-d bands into multiple transitions, producing the heavily-featured excitations into multiple transitions which can be deconvoluted in numerous Gaussian components.[S3] Details regarding transition assignments are collected in **Table S3**.

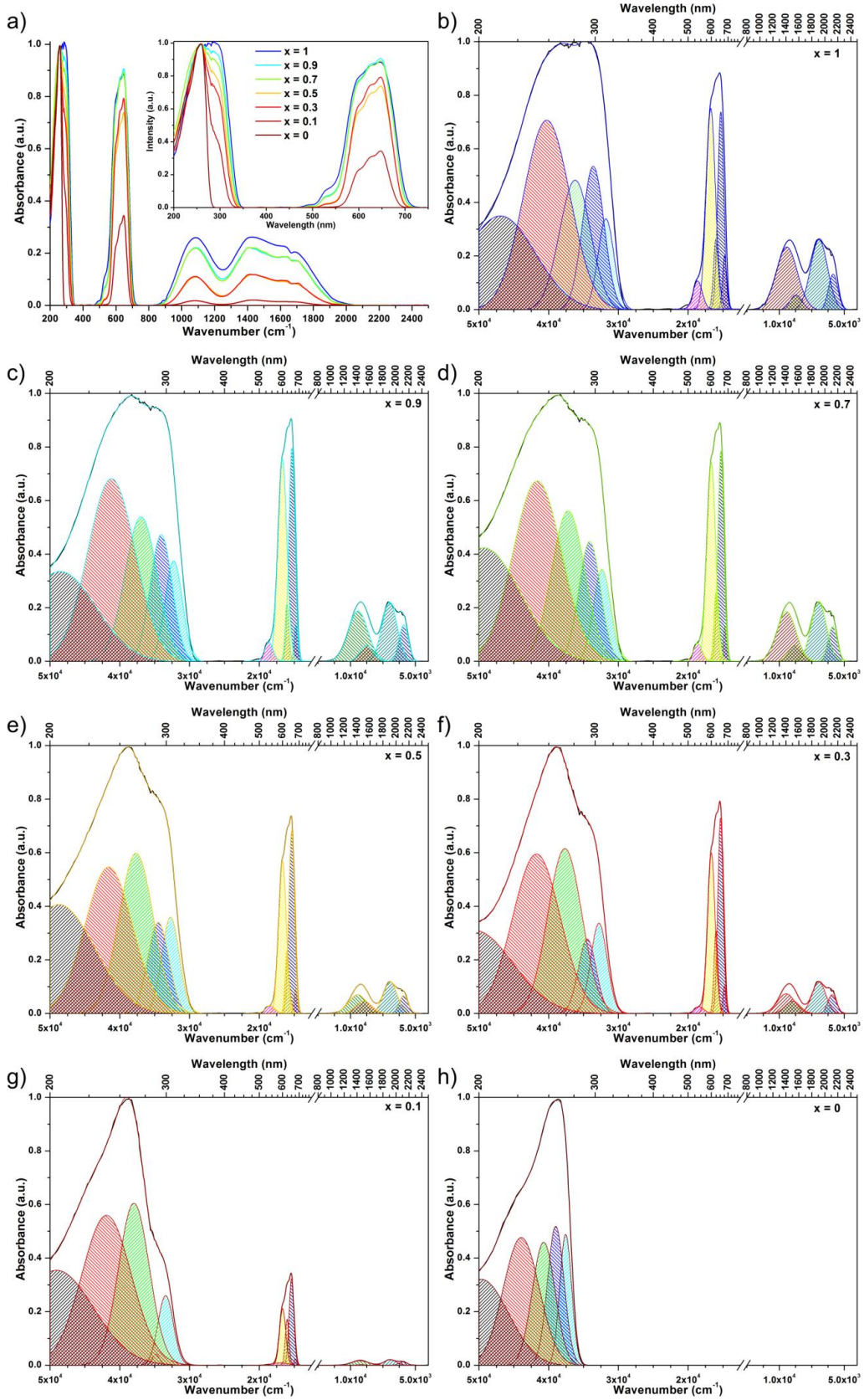

Figure S4. UV-Vis-NIR measurements results for pure compounds (**1-Co** and **0-Co**) and solid-solutions (**Co_xZn_{1-x}**).

Table S3. Results of deconvolution of UV-Vis-NIR spectra for pure (**1-Co** and **0-Co**) and solid-solutions (**Co_xZn_{1-x}**).

Compound	Peaks	Area	Centre		Width	Height	Compound	Peaks	Area	Centre		Width	Height
			$\tilde{\nu}$ (cm^{-1})	λ (nm)						$\tilde{\nu}$ (cm^{-1})	λ (nm)		
x = 1	**1**	4 439.9	46 938.1	213.0	10 041.5	0.353	**x = 0.9**	**1**	4 353.9	48 573.2	205.9	10 262.1	0.339
	2	5 933.0	40 290.7	248.2	6 665.4	0.710		**2**	5 834.6	41 213.4	242.6	6 797.7	0.685
	3	2 715.0	36 225.7	276.0	4 455.1	0.486		**3**	3 152.5	36 977.5	270.4	4 638.0	0.542
	4	2 086.2	33 617.6	297.5	3 093.8	0.538		**4**	1 881.1	34 072.3	293.5	3 155.5	0.476
	5	979.9	31 800.2	314.5	2 287.5	0.342		**5**	1 176.5	32 284.0	309.8	2 484.3	0.378
	6	172.8	18 645.5	536.3	1 314.9	0.105		**6**	106.4	18 646.0	536.3	1 201.7	0.071
	7	1 239.2	16 764.6	596.5	1 320.1	0.749		**7**	1 208.1	16 693.3	599.0	1 280.3	0.753
	8	221.2	16 025.0	624.0	675.3	0.261		**8**	146.8	16 034.5	623.7	548.9	0.213
	9	796.0	15 323.9	652.6	863.2	0.736		**9**	857.2	15 335.3	652.1	860.3	0.795
	10	145.6	14 760.6	677.5	583.5	0.199		**10**	80.4	14 766.0	677.2	476.7	0.135
	11	483.3	9 432.6	1 060.1	1 632.1	0.236		**11**	362.0	9 432.9	1 060.1	1 527.6	0.189
	12	66.4	8 724.1	1 146.3	933.3	0.057		**12**	76.6	8 768.4	1 140.5	1 011.1	0.060
	13	434.7	6 944.0	1 440.1	1 314.6	0.264		**13**	325.2	6 997.9	1 429.0	1 179.9	0.220
	14	121.7	5 860.0	1 706.5	721.0	0.135		**14**	122.4	5 904.5	1 693.6	713.2	0.137
x = 0.7	**1**	5 571.1	49 306.5	202.8	10 434.1	0.426	**x = 0.5**	**1**	5 213.2	48 753.6	205.1	10 197.4	0.408
	2	5 904.1	41 645.6	240.1	6 971.6	0.676		**2**	4 661.3	41 608.7	240.3	6 788.7	0.548
	3	3 353.1	37 216.4	268.7	4 750.0	0.563		**3**	3 679.9	37 677.8	265.4	4 900.9	0.599
	4	1 754.0	34 132.0	293.0	3 117.7	0.449		**4**	1 298.1	34 501.3	289.8	3 040.1	0.341
	5	1 066.6	32 357.5	309.0	2 462.9	0.346		**5**	1 132.6	32 740.9	305.4	2 508.4	0.360
	6	99.7	18 638.9	536.5	1 203.3	0.066		**6**	48.2	18 446.4	542.1	1 326.6	0.029
	7	1 171.2	16 700.1	598.8	1 261.1	0.741		**7**	780.9	16 682.5	599.4	1 100.5	0.566
	8	187.7	16 012.8	624.5	586.0	0.256		**8**	158.1	16 036.5	623.6	538.0	0.235
	9	820.7	15 316.5	652.9	833.8	0.785		**9**	681.1	15 373.6	650.5	798.2	0.681
	10	71.1	14 753.5	677.8	434.4	0.131		**10**	51.5	14 822.8	674.6	460.3	0.089
	11	346.7	9 458.6	1 057.2	1 477.8	0.187		**11**	121.6	9 457.7	1 057.3	1 378.2	0.070
	12	77.5	8 778.2	1 139.2	998.5	0.062		**12**	69.7	8 960.5	1 116.0	1 192.1	0.047
	13	332.0	6 974.7	1 433.8	1 191.3	0.222		**13**	156.8	6 946.7	1 439.5	1 059.9	0.118
	14	113.5	5 901.1	1 694.6	693.7	0.131		**14**	55.8	5 922.5	1 688.5	672.8	0.066
x = 0.3	**1**	4 259.3	50 596.2	197.6	10 937.0	0.311	**x = 0.1**	**1**	4 712.3	49 089.7	203.7	10 580.4	0.355
	2	5 098.9	41 759.1	239.5	6 824.2	0.596		**2**	4 981.6	41 913.3	238.6	7 096.8	0.560
	3	3 750.8	37 691.2	265.3	4 854.8	0.616		**3**	3 340.8	37 985.2	263.3	4 403.5	0.605
	4	894.1	34 486.2	290.0	2 562.8	0.278		**4**	53.2	34 836.6	287.1	1 025.4	0.041
	5	992.8	32 800.7	304.9	2 343.5	0.338		**5**	716.2	33 440.1	299.0	2 193.7	0.260
	6	42.4	18 413.3	543.1	1 346.7	0.025		**6**	24.3	17 007.6	588.0	2 263.7	0.009
	7	804.2	16 685.3	599.3	1 072.0	0.599		**7**	232.5	16 663.4	600.1	877.7	0.211
	8	216.5	16 021.2	624.2	561.7	0.308		**8**	115.8	16 019.3	624.2	539.2	0.171
	9	684.9	15 366.2	650.8	749.5	0.729		**9**	271.6	15 393.7	649.6	672.9	0.322
	10	54.9	14 808.4	675.3	427.0	0.103		**10**	11.2	14 840.4	673.8	378.6	0.024
	11	124.1	9 481.2	1 054.7	1 339.7	0.074		**11**	26.0	9 286.7	1 076.8	1 257.6	0.016
	12	66.6	8 983.4	1 113.2	1 143.8	0.046		**12**	1.5	9 164.6	1 091.2	672.9	0.002
	13	158.2	6 960.4	1 436.7	1 057.3	0.119		**13**	23.7	6 946.2	1 439.6	925.6	0.020
	14	59.3	5 942.6	1 682.8	675.3	0.070		**14**	9.3	5 959.7	1 677.9	619.8	0.012
x = 0	**1**	3 171.3	49 658.7	201.4	7 813.6	0.324							
	2	3 097.6	43 941.0	227.6	5 146.1	0.480							
	3	1 897.6	40 728.1	245.5	3 276.7	0.462							
	4	1 564.3	38 995.6	256.4	2 390.3	0.522							
	5	1 049.9	37 571.9	266.2	1 702.0	0.492							

Transitions assignment for peaks: **1** - **4** [$\pi \rightarrow \pi^*$, $n \rightarrow \pi^*$]; **5** [LMCT: $N_{pyridine} \rightarrow M^{II}$, M^{II} = Co, Zn]; **6** [$^4A_2 \rightarrow {}^4A_2$ (z)]; **7** - **10** [$^4A_2 \rightarrow {}^4B_2$, $^4B_1$ (x, y) for distorted Co(II) in two orientations]; **11** [$^4A_2 \rightarrow {}^4A_2$ (z)]; **12** and **13** [$^4A_2 \rightarrow {}^4B_2$, $^4B_1$ (x, y)]; **14** [$^4A_2 \rightarrow {}^4B_1$, $^4B_2$ (x, y)].

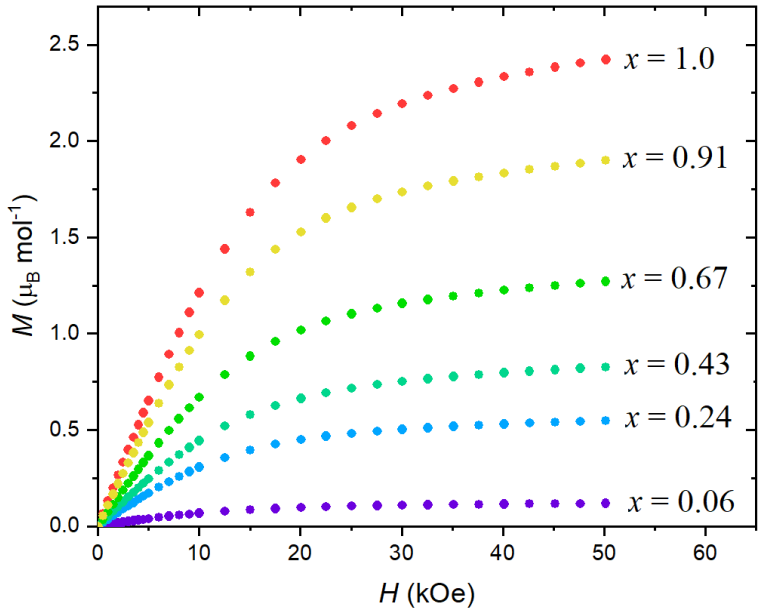

Figure S5. Magnetization vs. field dependence measured at 1.8 K for **1-Co** and **Co_xZn_{1-x}** compounds.

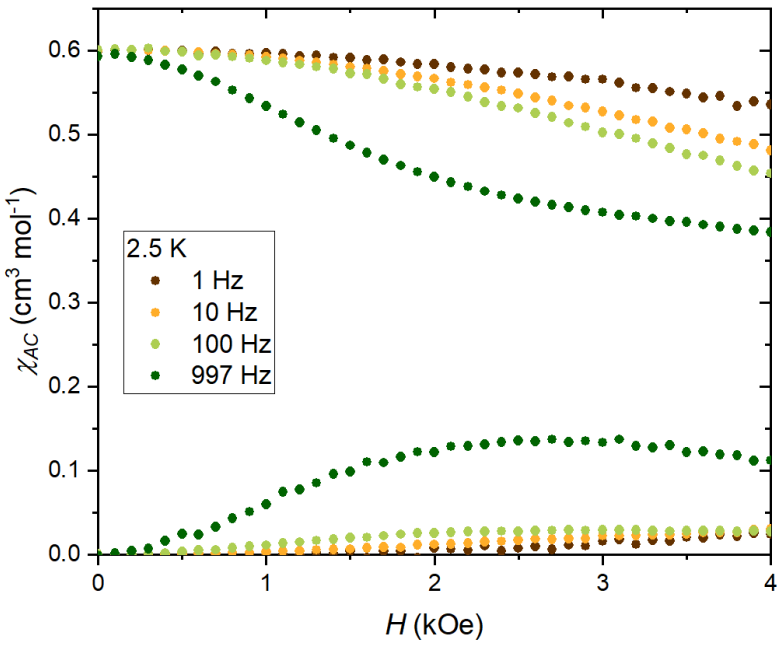

Figure S6. Field dependence of AC magnetic susceptibility for **1-Co** measured at 2.5 K and H_{AC} = 3 Oe at four different frequencies.

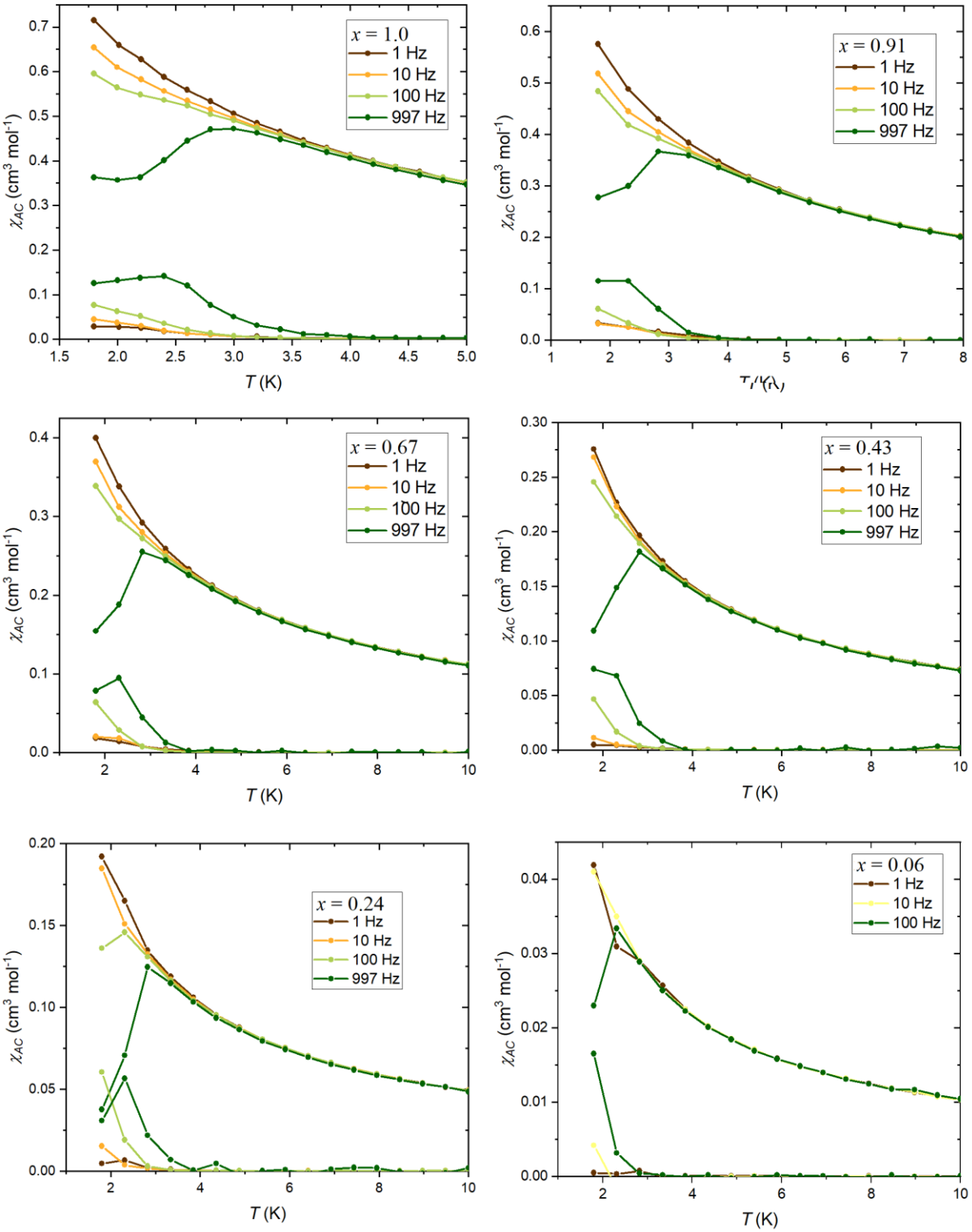

Figure S7. Temperature dependence of AC magnetic susceptibility for **1-Co** and **Co_xZn_{1-x}** measured at H_{DC} = 2.5 kOe and H_{AC} = 3 Oe at four different frequencies.

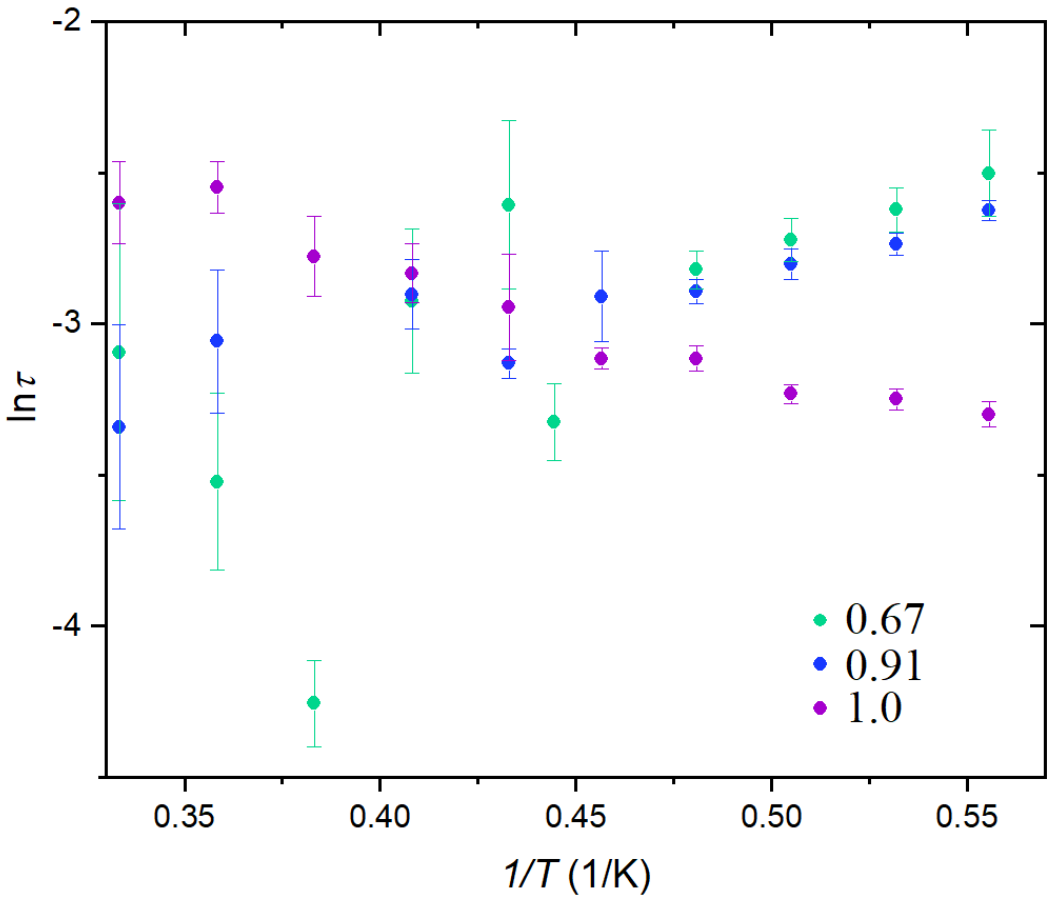

Figure S8. Arrhenius plot for *2. realxation step* of **1-Co** and $\mathbf{Co_xZn_{1-x}}$ with x = 0.67, 0.91, for dependences measured at H_{DC} = 2.5 kOe.

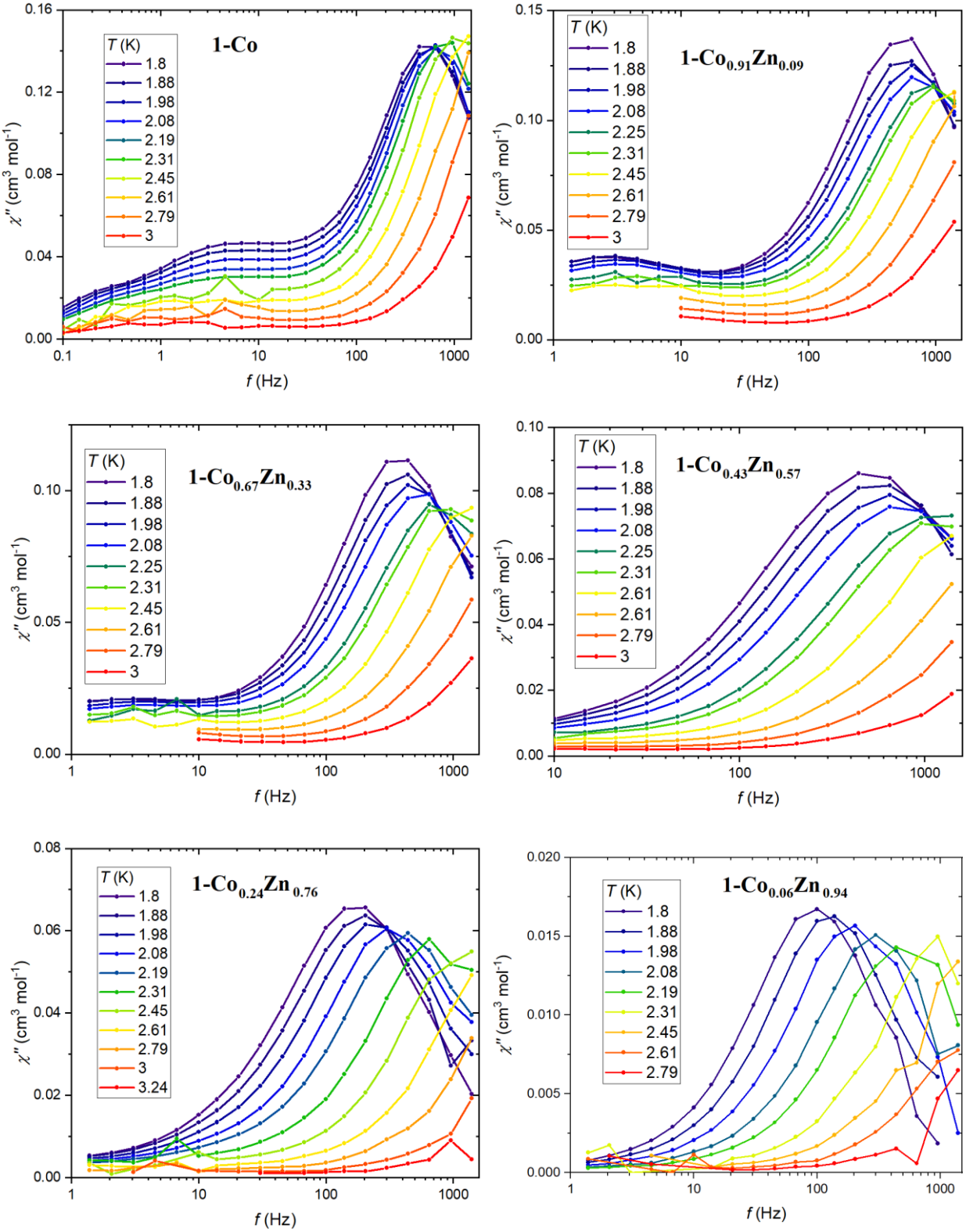

Figure S9. Frequency dependence of imaginary part of AC magnetic susceptibility, χ'', for **1-Co** and **Co_xZn_{1-x}** measured at 2.5 kOe and H_{AC} = 3 Oe at different temperatures. The shift of the maxima with the dilution is clearly visible. Solid lines are a guide to the eye.

Equation S1. The analytical formula obtained by applying generalized van Vleck formalism to determine full magnetic susceptibility tensor for the system with S = 3/2 for powder samples.[S4]

$$\frac{\beta^{-1}\chi_{ii}(\boldsymbol{h}_i)}{\mu_B^2} = g_{xi}^2\left[\frac{5}{4} - \frac{3(D+E)^2}{4\Delta^2}\left(1 - \frac{\tanh(\beta\Delta)}{\beta\Delta}\right) + \frac{D-3E}{2\Delta}\tanh(\beta\Delta)\right] + g_{yi}^2\left[\frac{5}{4} - \frac{3(D-E)^2}{4\Delta^2}\left(1 - \frac{\tanh(\beta\Delta)}{\beta\Delta}\right) + \frac{D+3E}{2\Delta}\tanh(\beta\Delta)\right] + g_{zi}^2\left[\frac{5}{4} - \frac{3E^2}{\Delta^2}\left(1 - \frac{\tanh(\beta\Delta)}{\beta\Delta}\right) + \frac{D}{\Delta}\tanh(\beta\Delta)\right];$$

$$\bar{\chi} = \frac{1}{3}[\chi_{xx}(\boldsymbol{h}_x) + \chi_{yy}(\boldsymbol{h}_y) + \chi_{zz}(\boldsymbol{h}_z)];$$

$$\Delta = \sqrt{D^2 + 3E^2};$$

$$\beta^{-1} = k_B T;$$

$\boldsymbol{h}$ **-** linearly independent configurations of the sampling field:

h_x = [1, 0, 0],h_y = [0, 1, 0], h_z = [0, 0, 1].

Table S4. Parameters obtained from fitting the double-mode Cole-Cole model to the AC magnetic susceptibility, χ' and χ'', vs. frequency, *f*, dependence measured for **1-Co.**

T	χ_0	$\Delta\chi_0$	χ_1	$\Delta\chi_1$	χ_2	$\Delta\chi_2$	τ_1	$\Delta\tau_1$	τ_2	$\Delta\tau_2$	α_1	$\Delta\alpha_1$	α_2	$\Delta\alpha_2$
K	**cm^3/mol**	**cm^3/mol**	**cm^3/mol**	**cm^3/mol**	**cm^3/mol**	**cm^3/mol**	**10^{-4} s**	**10^{-6} s**	**s**	**s**	**-**	**-**	**-**	**-**
1.80	0.2775	0.0017	0.2983	0.0038	0.1846	0.0038	2.829	2.1	0.0369	0.0016	0.0566	0.0065	0.456	0.011
1.88	0.2671	0.0014	0.2972	0.0031	0.1725	0.0030	2.654	1.7	0.0388	0.0014	0.0569	0.0053	0.4546	0.0090
1.98	0.2623	0.0012	0.2921	0.0025	0.1593	0.0025	2.535	1.3	0.0395	0.0013	0.0424	0.0045	0.4668	0.0082
2.08	0.2482	0.0018	0.3018	0.0033	0.1367	0.0030	2.251	1.7	0.0444	0.0019	0.0524	0.0060	0.448	0.012
2.19	0.2454	0.0015	0.2974	0.0026	0.1252	0.0023	2.067	1.3	0.0444	0.0016	0.0360	0.0047	0.460	0.010
2.31	0.2255	0.0095	0.3145	0.0135	0.0990	0.0094	1.607	6.0	0.0525	0.0093	0.049	0.024	0.442	0.056
2.45	0.2255	0.0065	0.3039	0.0080	0.0795	0.0042	1.226	3.3	0.0589	0.0058	0.037	0.014	0.434	0.033
2.61	0.226	0.012	0.290	0.013	0.0654	0.0046	0.850	4.3	0.0623	0.0083	0.026	0.019	0.458	0.042
2.79	0.234	0.011	0.270	0.012	0.0473	0.0021	0.577	3.1	0.0783	0.0068	0.016	0.014	0.433	0.029
3.00	0.279	0.019	0.208	0.020	0.0329	0.0023	0.417	4.8	0.074	0.010	0.010	0.023	0.478	0.041

Table S5. Parameters obtained from fitting the double-mode Cole-Cole model to the AC magnetic susceptibility, χ' and χ'', vs. frequency, *f*, dependence measured for **Co_xZn_{1-x}**, for x = 0.91**.**

T	χ_0	$\Delta\chi_0$	χ_1	$\Delta\chi_1$	χ_2	$\Delta\chi_2$	τ_1	$\Delta\tau_1$	τ_2	$\Delta\tau_2$	α_1	$\Delta\alpha_1$	α_2	$\Delta\alpha_2$
K	**cm^3/mol**	**cm^3/mol**	**cm^3/mol**	**cm^3/mol**	**cm^3/mol**	**cm^3/mol**	**10^{-4} s**	**10^{-6} s**	**s**	**s**	**-**	**-**	**-**	**-**
1.80	0.20187	0.00065	0.2937	0.0012	0.1195	0.0026	2.9523	0.87	0.0724	0.0024	0.0504	0.0024	0.312	0.011
1.88	0.1971	0.00090	0.2766	0.0016	0.1219	0.0031	2.713	1.2	0.0648	0.0025	0.0554	0.0034	0.315	0.013
1.98	0.1864	0.0014	0.2731	0.0023	0.1175	0.0041	2.432	1.6	0.0607	0.0031	0.0632	0.0049	0.321	0.018
2.08	0.1831	0.0013	0.2609	0.0020	0.1124	0.0031	2.184	1.3	0.0554	0.0022	0.0606	0.0044	0.323	0.015
2.19	0.1804	0.0039	0.2435	0.0063	0.113	0.011	1.785	3.3	0.0546	0.0082	0.041	0.014	0.400	0.046
2.31	0.1827	0.0018	0.2390	0.0026	0.0980	0.0034	1.630	1.4	0.0437	0.0022	0.0356	0.0059	0.362	0.019
2.45	0.1762	0.0041	0.2340	0.0054	0.0937	0.0063	1.195	2.6	0.0549	0.0064	0.032	0.012	0.394	0.034
2.61	0.1662	0.0072	0.232	0.012	0.12	0.10	0.798	3.0	0.13	0.34	0.017	0.021	0.49	0.17
2.79	0.1813	0.0032	0.2114	0.0038	0.0581	0.0064	0.540	1.1	0.047	0.012	0.0319	0.0062	0.371	0.033
3.00	0.192	0.011	0.191	0.012	0.0381	0.0065	0.343	2.6	0.035	0.012	0.039	0.015	0.335	0.057

Table S6. Parameters obtained from fitting the double-mode Cole-Cole model to the AC magnetic susceptibility, χ' and χ'', vs. frequency, *f*, dependence measured for $\mathbf{Co_xZn_{1-x}}$, for x = 0.67**.**

T	χ_0	$\Delta\chi_0$	χ_1	$\Delta\chi_1$	χ_2	$\Delta\chi_2$	τ_1	$\Delta\tau_1$	τ_2	$\Delta\tau_2$	α_1	$\Delta\alpha_1$	α_2	$\Delta\alpha_2$
K	**cm^3/mol**	**cm^3/mol**	**cm^3/mol**	**cm^3/mol**	**cm^3/mol**	**cm^3/mol**	**10^{-4} s**	**10^{-6} s**	**s**	**s**	**-**	**-**	**-**	**-**
1.80	0.1081	0.0014	0.2537	0.0025	0.0564	0.0057	4.059	3.3	0.082	0.012	0.0782	0.0061	0.249	0.053
1.88	0.10753	0.00073	0.2371	0.0015	0.0620	0.0032	3.701	1.7	0.0727	0.0054	0.0729	0.0036	0.296	0.027
1.98	0.10891	0.00065	0.2217	0.0015	0.0650	0.0032	3.377	1.5	0.0657	0.0048	0.0576	0.0036	0.352	0.025
2.08	0.10207	0.00073	0.2184	0.0014	0.0589	0.0026	2.833	1.3	0.0596	0.0037	0.0657	0.0037	0.330	0.023
2.19	0.0989	0.0034	0.2088	0.0048	0.0436	0.0049	2.120	4.3	0.0360	0.0046	0.064	0.014	0.231	0.070
2.31	0.0969	0.0031	0.2051	0.0048	0.0583	0.0092	1.805	3.4	0.074	0.021	0.055	0.013	0.383	0.074
2.45	0.0944	0.0048	0.1973	0.0061	0.0457	0.0067	1.242	3.7	0.054	0.013	0.041	0.016	0.362	0.076
2.61	0.0975	0.0033	0.1862	0.0038	0.0214	0.0027	0.796	1.8	0.0142	0.0021	0.0434	0.0089	0.172	0.064
2.79	0.1046	0.0049	0.1701	0.0053	0.0241	0.0041	0.472	1.9	0.0296	0.0087	0.0603	0.0097	0.267	0.062
3.00	0.1269	0.0071	0.1369	0.0075	0.0227	0.0051	0.319	2.3	0.0454	0.023	0.040	0.014	0.380	0.067

Table S7. Parameters obtained from fitting the double-mode Cole-Cole model to the AC magnetic susceptibility, χ' and χ'', vs. frequency, *f*, dependence measured for $\mathbf{Co_xZn_{1-x}}$, for x = 0.43**.**

T	χ_0	$\Delta\chi_0$	χ_1	$\Delta\chi_1$	τ_1	$\Delta\tau_1$	α_1	$\Delta\alpha_1$
K	**cm^3/mol**	**cm^3/mol**	**cm^3/mol**	**cm^3/mol**	**10^{-4} s**	**10^{-6} s**	**-**	**-**
1.80	0.0450	0.0020	0.2250	0.0026	3.159	4.9	0.1654	0.0068
1.88	0.0483	0.0026	0.2105	0.0033	2.928	6.1	0.1538	0.0091
1.98	0.0481	0.0025	0.2012	0.0032	2.574	5.5	0.1536	0.0089
2.08	0.0485	0.0029	0.1908	0.0035	2.153	5.4	0.1440	0.0097
2.19	0.0405	0.0046	0.1860	0.0052	1.422	5.8	0.144	0.013
2.31	0.0490	0.0047	0.1731	0.0053	1.276	5.5	0.123	0.014
2.45	0.0425	0.0090	0.1694	0.0095	0.783	6.5	0.116	0.019
2.61	0.037	0.019	0.166	0.020	0.433	7.7	0.125	0.026
2.79	0.037	fixed	0.15619	0.00038	0.237	9.4	0.133	0.016
3.00	0.037	fixed	0.14694	0.00031	0.995	8.5	0.186	0.024

Table S8. Parameters obtained from fitting the double-mode Cole-Cole model to the AC magnetic susceptibility, χ' and χ'', vs. frequency, *f*, dependence measured for $\mathbf{Co_xZn_{1-x}}$, for x = 0.24**.**

T	χ_0	$\Delta\chi_0$	χ_1	$\Delta\chi_1$	τ_1	$\Delta\tau_1$	α_1	$\Delta\alpha_1$
K	**cm^3/mol**	**cm^3/mol**	**cm^3/mol**	**cm^3/mol**	**10^{-4} s**	**10^{-6} s**	**-**	**-**
1.80	0.0245	0.0010	0.1656	0.0015	9.68	13	0.1449	0.0066
1.88	0.0215	0.0018	0.1618	0.0027	8.09	19	0.160	0.012
1.98	0.0207	0.0013	0.1555	0.0018	6.49	11	0.1511	0.0078
2.08	0.0180	0.0019	0.1510	0.0024	4.71	11	0.150	0.011
2.19	0.0196	0.0023	0.1438	0.0028	3.627	9.9	0.136	0.013
2.31	0.0171	0.0050	0.1386	0.0059	2.130	1.3	0.128	0.023
2.45	0.0190	0.0067	0.1278	0.0073	1.234	9.7	0.094	0.025
2.61	0.0062	0.014	0.134	0.015	0.582	9.2	0.115	0.028
2.79	0.0062	fixed	0.12796	0.00042	0.294	1.6	0.127	0.021
3.00	0.0062	fixed	0.12050	0.00041	0.138	1.7	0.117	0.039

Table S9. Parameters obtained from fitting the double-mode Cole-Cole model to the AC magnetic susceptibility, χ' and χ'', vs. frequency, *f*, dependence measured for $\mathbf{Co_xZn_{1-x}}$, for x = 0.06**.**

T	χ_0	$\Delta\chi_0$	χ_1	$\Delta\chi_1$	τ_1	$\Delta\tau_1$	α_1	$\Delta\alpha_1$
K	**cm^3/mol**	**cm^3/mol**	**cm^3/mol**	**cm^3/mol**	**10^{-4} s**	**10^{-6} s**	**-**	**-**
1.80	0.00574	0.00034	0.03636	0.00055	16.80	31	0.044	0.012
1.88	0.00475	0.00013	0.03590	0.00020	12.000	8.1	0.0631	0.0040
1.98	0.00489	0.00035	0.03405	0.00052	8.19	15	0.048	0.012
2.08	0.00526	0.00033	0.03206	0.00046	5.226	8.8	0.0415	0.0099
2.19	0.00403	0.00028	0.03209	0.00035	3.260	4.5	0.0608	0.0068
2.31	0.00511	0.00097	0.0292	0.0012	1.786	8.0	0.029	0.021
2.45	0.0051	0.0028	0.0270	0.0030	0.92	12	0.005	0.042
2.61	0.0092	0.0055	0.0218	0.0056	0.57	20	0.061	0.067
2.79	0	fixed	0.02900	0.00020	0.240	3.0	0.004	0.054

References:

[S1] A. M. Majcher, P. Dąbczyński, M. M. Marzec, M. Ceglarska, J. Rysz, A. Bernasik, S. Ohkoshi and O. Stefańczyk, *Chem. Sci.*, 2018, **9**, 7277–7286.
[S2] H. Ishihara, M. Nakashima, H. Nakashima, R. Tateno, Y. Shibamura, T. Makino, A. Kikuchiu, D. Kii, K. Horiuchi, I. Svoboda, H. Fuess, H. Terao, *Z. Naturforsch., B: Chem. Sci.* (2011), **66**, 27.
[S3] J. M. Zadrozny, J. Telser, J. R. Long, *Polyhedron*, 2013, **64**, 209-217.
[S4] R. Pełka, *ACTA PHYSICA POLONICA A*, 2011, **119**, 428–436.